

# A Flow-Through Cell for *in situ*, Real Time X-ray Absorption Spectroscopy Studies of Geochemical Reactions

By John E. Villinski, Peggy A. O'Day, Tim L. Corley and Martha H. Conklin

## ABSTRACT

The contact of acid mine waste with mineral surfaces can result in a series of complex geochemical reactions, including mineral precipitation and dissolution, which are often kinetically controlled processes. One problem in formulating rate expressions for dissolution/precipitation reactions is that intermediate species are often formed. Identification of these species can lead to more accurate models, and hence, better predictions of the fate of the various chemical species. The use of spectroscopic probes to directly identify chemical species often requires high vacuum, which can induce modifications in surfaces and surface species. Synchrotron X-ray absorption spectroscopy is an element-specific method which can be used to probe samples in an aqueous environment. We developed a flow-through reaction cell for use at the Stanford Synchrotron Radiation Laboratory (SSRL), Stanford CA, that allowed for spectroscopic probing of minerals undergoing precipitation or dissolution reactions. This cell, coupled with X-ray absorption near-edge structure (XANES) spectroscopy, allowed us to detect the changes in elemental speciation of manganese during the reductive dissolution of  $MnO_2$  by Fe(II). The use of this flow-through reaction cell will allow for the coupling of spectroscopic measurements of elemental oxidation states with conventional rate measurements.

## INTRODUCTION

The Pinal Creek Basin, near Globe, AZ, has been impacted by an acidic, suboxic plume originating from wastes produced by the copper mining industry. The plume is characterized by high concentrations of ferrous iron and sulfate, as well as elevated concentrations of other heavy metals. The Fe(II) reductively dissolves the manganese (hydr)oxide coatings from the alluvial aquifer material, releasing Mn(II) to the aqueous phase, and precipitating a ferric iron phase. The acid in the plume is retarded due to 0.34 percent carbonate by weight in the alluvial material (Eychaner and Stollenwerk, 1989). For a more complete description of the site, the reader is referred to Eychaner (1991).

Stollenwerk (1994) conducted column experiments using natural sediments with uncontaminated and contaminated groundwater. The effluent profile of Mn(II) was a sharp spike followed by a very slow tail towards influent conditions. In addition, the total release of Mn(II) over an experiment lasting 30 pore volumes was only 46% of the amount that would be predicted by the amount of Fe precipitated and the stoichiometry of the following reaction:



Stollenwerk, (1994) found that the transport of Mn(II) through the basin could not be modeled adequately using equilibrium principles.

Results from batch experiments performed at the University of Arizona with MnO<sub>2</sub>-coated quartz and artificial acid mine drainage (AAMD) were similar to those from column experiments done by Stollenwerk (1994) in that there was an initial fast release of Mn(II), followed by a drastically slower release as the week-long experiment continued. In addition, the proportion of Fe(II) consumed to Mn(II) released increased as the experiment progressed.

Stollenwerk (1994) proposed that the discrepancy between the amount of Mn released and the amount predicted to be released was due to Mn remaining associated with the solid phase, either coprecipitated with Fe or that the Mn(IV) was incompletely reduced. No known Mn phase was identified in the reacted sediments using X-ray diffraction (XRD) (Lind and Stollenwerk, 1995).

Other researchers have proposed the existence of an intermediate phase in the reduction of Mn(IV) (hydr)oxides (Jardine and Taylor, 1995; Kozawa and Yeagar, 1965; Perez-Benito and others, 1996). Few studies have actually detected the presence of Mn(III). Giovanoli and others, (1971) detected the presence of manganite in samples of birnessite reduced by cinnamyl alcohol using electron microscopy. Crowther and others, (1983) detected Mn(III) at the surface of birnessite reacted with Co(II) using X-ray photoelectron spectroscopy (XPS). Likewise, the presence of Mn(III) was detected on the surface of birnessite reduced in the presence of As(III) using XPS (Nesbitt and others, 1998).

One problem with the use of these high vacuum techniques (XPS, SEM) is the fact that the mineral surface is removed from the environmental state as it is dried prior to analysis. Synchrotron X-ray absorption spectroscopy (XAS), on the other hand, allows for spectral analysis of elements in a complex matrix and in the presence of an aqueous solution.

XAS is an element-specific probe that has the advantages over other spectroscopic techniques including low detection limits (as low as 10-100 ppm depending on the element and the matrix), and the ability to probe samples of varying phases (crystalline or amorphous solids, gases and liquids) (Brown and others, 1988). XAS also provides a unique spectral signal for each local environment of the element of interest (Brown and others, 1988). For a more complete review of XAS the reader is referred to Brown and others (1988).

The focus of this paper is on the design of a flow cell for XAS that can be used in a fluorescence detector at the Stanford Synchrotron Radiation Laboratory (SSRL). XAS is generally separated into two parts, the extended X-ray absorption fine structure (EXAFS) and the X-ray absorption near-edge structure (XANES). In this study we used the XANES portion of the spectra to shorten the acquisition time for data acquisition in order to monitor changes in the oxidation state during the dissolution reaction.

The system we chose to study was the geochemical reactions that occur in the alluvial aquifer at Pinal Creek. The system was simplified significantly from the natural state. This was done to focus on the Mn/Fe redox couple, rather than other possible competing reactions. Thus synthetic materials were used which allow for better pH control and a more complete description of the mineral surfaces. Likewise, other trace metals were excluded from the solution to minimize other surface reactions (sorption, precipitation) that might compete with the Mn/Fe redox reactions.

## EXPERIMENTAL PROCEDURES

### Materials

All chemicals used were reagent grade. The solid materials used for the flow experiments conducted at the SSRL was a MnO<sub>2</sub>-coated silica gel. The silica gel was SiLCRON G-604 (SCM Corporation) with a nominal grain size of 13.5 μm, a specific surface area of 320 m<sup>2</sup> g<sup>-1</sup>, a specific gravity of 2.1 g cm<sup>-3</sup>, and a dry bulk of 0.18 g cm<sup>-3</sup> (SCM Corp. technical data sheet). Fine particles (< 1 μm) were removed by suspending the material in purified water (Milli-RO 6 plus/Milli-Q plus reagent water system Millipore Corp., USA, with a resistivity of 10<sup>-18</sup> MΩ cm, referred to herein as Milli-Q) in a 0.4 m high cylinder, and allowing it to settle for 24 hours. This process was continued until the supernatant was free of fine particles.

A rigorous cleaning process was used to remove surface contaminants from the silica gel. Following a wash with Milli-Q, the silica gel was refluxed with 2 M HNO<sub>3</sub> (trace metal grade, Fisher Scientific) for two hours. This was followed by rinsing with Milli-Q until the conductivity of the

effluent was equal to that of the influent, and finally, the silica gel was dried at 105°C.

The silica gel was then coated with a Mn(IV) oxide using a modification of a dry oxidation procedure of Mn(NO<sub>3</sub>)<sub>2</sub> (J. T. Baker, Inc.) (Stahl and James, 1991; Covington and others, 1962). A measured mass of silica gel was placed in a teflon vessel. Mn(NO<sub>3</sub>)<sub>2</sub> was added to the vessel in an amount that would yield a desired MnO<sub>2</sub> concentration, and then Milli-Q was added to allow the Mn(NO<sub>3</sub>)<sub>2</sub> to be mixed evenly through the solid. The vessel was then placed in an oven at 105°C and allowed to dry. During the initial drying process, the solid/liquid mixture was stirred every 10-15 minutes to prevent the salts from wicking. After 24 hours, the dried solids were baked at 160°C for 72 hours.

After cooling, the Mn(IV)-coated silica was placed in 250 ml polyethylene bottles and filled with Milli-Q. The bottles were placed on their sides, and placed on a shaker table over night. The supernatant was decanted, and the procedure was repeated until the supernatant was free of visual Mn(IV) oxides (referred to herein as MnO<sub>2</sub>). This allowed for the removal of easily “sloughed-off” MnO<sub>2</sub>. The average valence of the Mn in the MnO<sub>2</sub>-coated silica was determined to be 4.01±0.02 by the oxalate method (Hem, 1980). The MnO<sub>2</sub> concentration of the MnO<sub>2</sub>-coated silica gel was 14.4 mg MnO<sub>2</sub> g<sup>-1</sup> total, or 0.91% Mn by weight.

All solutions were made with Milli-Q water that had less than 10 µg/l dissolved oxygen (DO), measured using an Hach DR100 spectrophotometer with low-range DO AccuVac vials (detection limit: 10 µg/l, Hach Co.). To accomplish this, Milli-Q water was boiled for at least five minutes, cooled under a constant stream of N<sub>2</sub> gas, and then placed in a glove box (Coy Laboratory Products), and exposed to a 97% N<sub>2</sub>-3% H<sub>2</sub> atmosphere for at least five days. The FeSO<sub>4</sub>·7H<sub>2</sub>O (Aldrich Chemical Co., Inc.) was stored in the N<sub>2</sub>-H<sub>2</sub> atmosphere to prevent oxidation of the Fe(II). The composition of the solutions are listed in Table 1. The pH of the solutions were adjusted with either HNO<sub>3</sub> or NaOH (Fisher Scientific) solutions standardized against known quantities of potassium hydrogen phthalate (MCB Manufacturing Chemists, Inc.).

**Table 1.** Chemical composition of contaminated groundwater from Pinal Creek and solutions used

in flow-through experiments. All values in mmol expect for pH (standard units) and temperature (°C).

Constituent	Cont. GW*	Inert elect.**	Reactive solution
pH	3.30	3.00	3.00
Temperature	17	25	25
Dissolved O <sub>2</sub>	<0.006	<0.0004	<0.0004
Ca	11.6	6.3	6.3
Mg	15.8	93.7	82.7
Na	9.4	9.5	9.5
K	0.2	0	0
Fe	52.4	0	11.0
Mn	1.34	0	0
Al	10.5	0	0
Cu	2.4	0	0
Co	0.20	0	0
Ni	0.06	0	0
Zn	0.33	0	0
SO <sub>4</sub> <sup>2-</sup>	100	102	102
Cl	9.5	9.5	9.5
Ionic Strength	232	220	220

\* Contaminated groundwater, values from Stollenwerk (1994)

\*\* Inert electrolyte

## Flow Cell Design

The incoming X-ray beam at the SSRL has a horizontal profile that is 20 mm wide and is usually slit down to 1-2 mm high. The design of the cell was made with this in mind (Figure 1). The flow cell was constructed of polycarbonate. The bed support was made from a porous sheet of ultra-high molecular weight (UHMW) polypropylene with pore size ranging from 10-20 µm (X-4920, Porex Technologies). The bed support was treated with concentrated H<sub>2</sub>SO<sub>4</sub> to make the surfaces hydrophilic. The windows consisted of Kapton tape with an acrylic adhesive. The tubing connections to the cell were made by threading 1/16” O.D. PEEK tubing with a 1-72 die, and tapping the cell inlet, outlet and ports.

## Experimental Design

The experimental set-up is shown in Figure 2. All tubing other than the PEEK tubing that was directly connected to the cell was either Teflon (0.020" I.D.) or Tygon (0.030" I.D.). The solution was delivered with a Ismatec IPN peristaltic pump (Ismatec SA) at flow rates from  $50\text{--}125\ \mu\text{l min}^{-1}$ .

Micro pH and reference electrodes with  $3\ \mu\text{l}$  dead volumes were used to monitor effluent pH (Microelectrodes, Inc.). The effluent was then collected in set fraction sizes using a Frac100 fraction collector (Pharmacia). The fractions were then analyzed for Mn(II) and total Fe ( $\text{Fe}_T$ ) by flame AA.

The cell was packed with the  $\text{MnO}_2$ -coated silica gel, which was kept wet at all times. The cell was packed wet by attaching a syringe filled with  $\text{MnO}_2$ -coated silica gel and Milli-Q to the outlet port of the cell, and allowing gravity to pack the cell.

In order to prevent oxygen entering into solution during the experiment, the solutions as well as the sample chamber of the fluorescence detector were purged continually with ultra-high purity He gas.

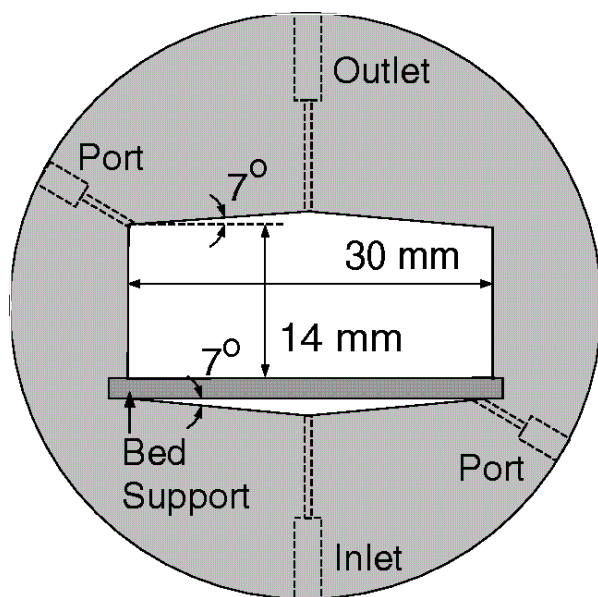


**Figure 1.** Plan view of the flow cell used at SSRL. The cell was constructed of 3 mm thick

polycarbonate. The bed support was constructed from a porous sheet of 1/16" thick UHMW polypropylene. The inlet, outlet and side ports were all tapped to accept a 1-72 thread size. Dashed lines indicate elements that are internal to the cell.

Experiments with this cell differ from those of a normal column experiment. Firstly, the cell is not rigid due to the fact that Kapton windows can stretch. Thus the dimensions of the cell can change due to pressure changes within the cell. Because of this, the experiments have been run as a fluidized bed-reactor with no filter constraining the top of the bed. With a filter on top of the packed bed, pressure can build up within the cell, causing the windows to stretch outward. At this point, channeling can occur within the bed.

Conversely, with no confining filter on top of the bed, other problems can occur such as loss of bed material from the cell from changes in solution composition or increases in flow rate, or a siphoning action which can occur when moving the cell in and out of the detector chamber (thus changing the head in the system). Keeping all parts of the system from the cell to the fraction collector at the same elevation helped to mitigate siphoning.

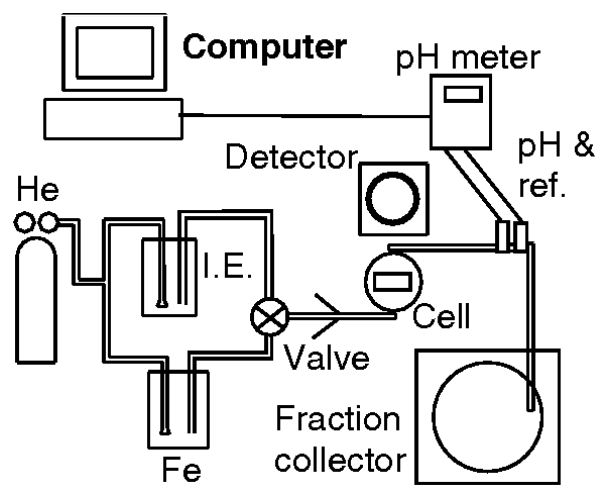


**Figure 2.** Experimental design. Ultra high purity He was used to sparge the solutions to prevent  $\text{O}_2$  from entering the cell. **I.E.** stands for inert electrolyte, and **Fe** is the 11 mM Fe(II) solution. **pH and ref.** refers to the in-line pH and reference electrodes.

Secondly, the dead volume of the cell is large compared to the pore volume due to the size of the X-ray hutches at SSRL, and the placement of the ion and fluorescence detectors. The estimated pore volume of a normal experiment was on the order of 350  $\mu\text{l}$ . The dead volume was estimated to be 1760  $\mu\text{l}$ , which is a factor of five greater than the pore volume and therefore the majority of the dispersion could occur in the dead volume as opposed to the bed.

Therefore the determination of the dispersive properties of the system are not as straight forward as with a conventional column experiment. The performance and dispersive properties of the system were characterized in the laboratory prior to experiments at SSRL. A tracer test was conducted with the packed cell by changing the ionic strength of the influent inert electrolyte solution from 5 mM to 10 mM  $\text{CaSO}_4$  and monitoring the conductivity with an Altech 320 conductivity detector (Altech Associates, Inc.).

## XAS Data collection

All spectra were collected at the SSRL (Stanford, CA) on wiggler beam lines IV-1 and IV-3. Beam current ranged from 30-90 mA at 3 GeV and the magnetic field of the wiggler was 18 kG. Either Si(111) or Si(220) monochromators were used with an unfocused beam. The monochromators were detuned such that the incoming beam flux was reduced by 30-50% to reject higher-order harmonic reflections. Energy was calibrated by assigning the first inflection of the absorption edge of Mn metallic foil to 6539 eV.

Fluorescence spectra were collected with the sample at a  $45^\circ$  angle to the incident beam using a Stern-Heald-type detector (Lytle and others, 1984) with Soller slits and a Cr filter to reduce background scattering and fluorescence.

Transmission spectra of the reference compounds were collected using two gas-filled ion chambers.

After beam alignment and energy calibration, the sample in the flow cell was placed in the path of the beam with an inert electrolyte solution flowing at a predetermined flow rate. A

background spectrum was then recorded. Next the flow was switched to the reactive Fe(II) solution and spectra were collected for two hours as the reaction progressed. The pH was recorded and the effluent was collected in fractions.

All the XANES spectra were treated in the same manner. The background was subtracted from the spectrum using a low-order polynomial fit over the pre-absorption edge region of 6520-6533 eV using the computer program EXAFSPAK (George, 1995).

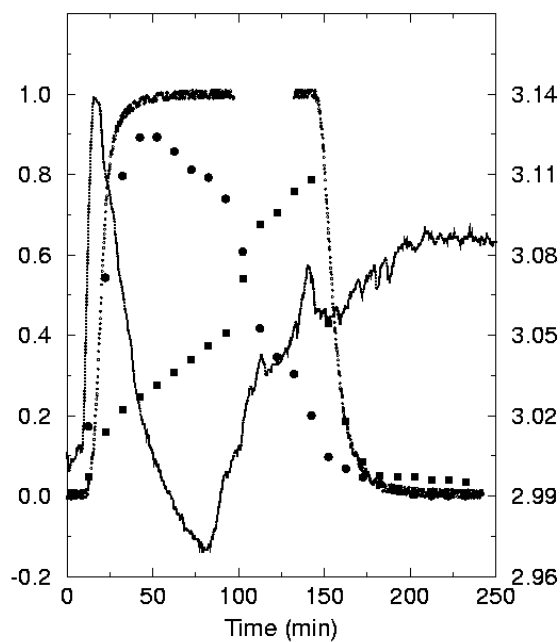
## RESULTS AND DISCUSSION

### Cell Characteristics

Results of the aqueous phase data are shown in figure 3. The salt tracer break-through curve (BTC) is asymmetric, with significant tailing as the normalized concentration approaches a value of one. This type of behavior is often attributed to diffusion-limited mass transfer to immobile regions of the pore volume (van Genuchten and Wierenga, 1976). This is expected as the silica gel has a significant internal porosity. The porosity of the  $\text{MnO}_2$ -coated silica gel under static conditions was determined to be 74%. Assuming a 42% external porosity (representative porosity for clay-sized particles, Todd, 1980), then 43% of the pore volume would be internal pores, or immobile.

The pH BTC shows an initial increase in pH indicating that the  $\text{MnO}_2$  coating is being reductively dissolved by the Fe(II). The subsequent precipitation of the resulting Fe(III) can be noted to occur fairly rapidly, as the pH starts to decrease at approximately 16 minutes. The pH continues to decrease until approximately 80 minutes into the experiment and then slowly increases back above the starting pH. This drift in the pH was probably due to some solid accumulating on the porous frit of the pH electrode. After cleaning the pH electrode returned to normal operation.

**Figure 3.** Breakthrough curves for flow-through



reaction conducted at SSRL and tracer experiment conducted in the laboratory. The dots are the tracer data, the circles are the Mn(II) data, the squares are  $Fe_T$  data and the continuous line is the pH data. The  $Fe_T$  data was normalized to the influent Fe(II) concentration of 11 mM, and the Mn(II) data was normalized to a concentration of 5.5 mM as the stoichiometry of the reaction requires two Fe(II) to reduce one Mn(IV). The tracer was normalized to a conductivity of one.

The Mn(II) BTC indicates that, initially, the reaction is not kinetically limited. However, as time progresses, the tailing present in the down-sloping portion of the  $Mn_T$  BTC suggests a kinetically limited reaction. The deviation of the Mn(II) BTC from the tracer BTC as the tracer BTC approaches a normalized concentration of one could also be due to kinetic limitations.

The apparent early release of Mn(II) as compared to the tracer at 12 mins, as well as the early change in pH, was probably due to the siphoning action mentioned earlier. The effect of the siphoning would have decreased the pressure within the cell. This would lead to a smaller cell volume as the Kapton windows were drawn inward. This would decrease the total dead

volume, and therefore the travel time from the control valve to the fraction collector would decrease. A decrease in the cell volume of 0.35 ml could explain the early release of Mn(II) and the early rise in pH. This would translate to a 25% decrease in the cell volume, not an unreasonable amount given the degree to which the Kapton tape can stretch.

The Fe(II)/Fe(III) in the effluent starts to increase slowly, and this increase coincides with both the deviation of the Mn(II) BTC from the tracer BTC and the start of the Fe(III) precipitation as noted by the decreasing pH. The overall  $Fe_T$  BTC mirrors that of the Mn(II) BTC, which is expected. The desorption portion of the  $Fe_T$  BTC, like the sorption portion of the Mn(II) BTC, occurs before the tracer BTC, and could be due to reduced cell volume. Significant tailing is noted after 160 minutes, and this is probably due to the desorption of Fe(II) and/or Fe(III) from the newly formed ferric precipitates. Fe(III) is slightly soluble at pH 3.

## XANES Data

Figure 4 shows the series of spectra collected on the same cell described above. For visual comparison, the spectra have been normalized to a value of one for the absorption edge height. The absorption edge height, which is related to the overall Mn concentration, actually decreased from 2.52 to 0.30 absorption units (arbitrary units) over the two hours the spectra were collected. This corresponds approximately to an one-order-of-magnitude decrease in total Mn concentration.

From figure 4, two trends can be noted. First is that the shoulder at 6554 eV increases as the experiment progresses. This is consistent with the release Mn(II) into the aqueous phase and the corresponding absorption maximum for an  $MnSO_4$  solution at 6554 eV. The release of Mn(II) to the aqueous phase is known from the solution data.

The second notable feature in figure 4 is the shift in the position of maximum absorption to a lower energy as the reaction progresses. This would not be expected if the spectra were composed only of our two known spectra, the starting Mn mineral ( $MnO_2$ ), and the Mn(II) solution.

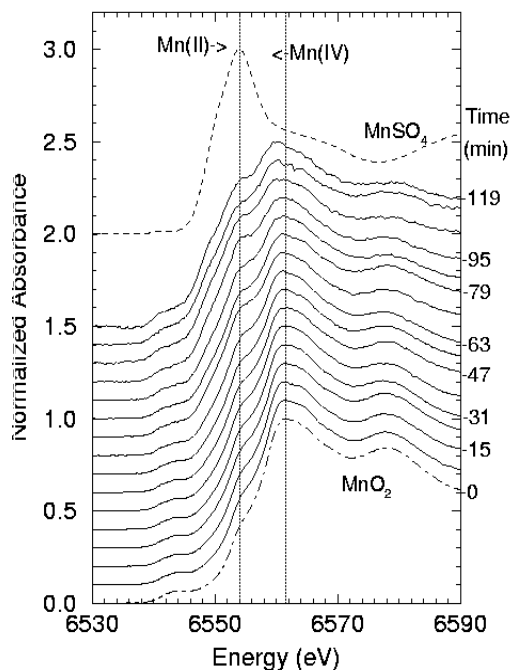


**Figure 4.** XANES spectra collected during the reductive dissolution of  $\text{MnO}_2$  by  $\text{Fe(II)}$ . The dot-dash line is the spectra of the original  $\text{MnO}_2$  and the dashed line is the spectra of an  $\text{MnSO}_4$  solution. For visual clarity, the spectra have all been normalized to an edge height of one, and the individual spectra have been shifted upward indicating a progression in time.

This suggests the presence of another Mn phase. An argument can be made that this phase could contain Mn(III). The shape of the XANES spectra is dependent on the valence of the element as well as on the short- and long-range order around the Mn atoms. Studies of XANES data indicate that the absorption edge (1st inflection point) and the  $1s - 4p$  peak (energy of maximum absorption) of the transition metals shifts to a lower energy as the valence decreases (Wong and others, 1985; Qi-wu and Wong, 1984).

While the manganese minerals that we have studied exhibit a general decrease in absorption maximum with lower oxidation state, the range of absorption maximum for a particular oxidation state is fairly wide. The ranges of absorption maximum for the the II, III and IV oxidation states overlap each other. The range of maximum absorption for

Mn(III) and Mn(IV) oxides we have studied are 6557.7-6561.2 and 6560.2-6562.3 eV, respectively.

The absorption maxima shifted from 6561.6 to 6560.3 during the course of the experiment. This shift in the energy of maximum absorption could be due to either the formation of Mn(III) or the rearrangement of the Mn(IV) oxide structure. Fitting the reaction spectra with spectra of reference compounds (e.g., well-characterized Mn minerals) indicate the presence of an hausmannite-like phase is present during the reaction (Villinski and others, 1999)

## CONCLUSIONS

We have demonstrated that the flow-through reaction cell constructed for use at SSRL is a valuable tool for studying complex geochemical reactions at the molecular level. This configuration not only allows for the identification of reaction intermediates, but also provides kinetic information of the formation and destruction of these reaction intermediates through the spectroscopic probing of the system *in situ* and in real time.

The one minor drawback of the system as designed is the fact that the cell is not rigid due to the use of Kapton tape for the window materials. This allows for the cell volume to change and thus the interpretation of effluent data is qualitative rather than quantitative. The use of a very thin window made of a low molecular weight material is necessary in order to maintain the low detection limit of the instrument due to absorption of the X-ray beam and the fluorescence signal by the window.

Various changes could be made to the cell design that would overcome this limitation. The windows of the cell could be made with either a thicker Kapton window (0.005") that was actually glued in place or with beryllium. The thicker Kapton window would decrease the incoming X-ray flux by approximately 15 % (from 96% transmission to 82 %), but would increase the rigidity of the window. A beryllium window would obviate this loss of flux, with 96% transmission for a thickness of 0.005", similar to that of a Kapton window of 0.001" thickness, albeit with a higher cost.

This experimental approach yields information about complex geochemical systems that are not available from conventional bench-scale laboratory experiments. The coupling of information from these *in situ* real-time XAS experiments with conventional batch experiments can provide the improved formulation of reaction rate equations and lead to better predictions of the fate and transport of trace metals in aqueous environments.

## ACKNOWLEDGEMENTS

This publication was made possible by grant number P42 ESO4940 from the National Institute of Environmental Health Sciences with funding provided by EPA and the National Science Foundation (grant NSF-EAR-962-9276 to P.A. O'Day). Work done (partially) at SSRL which is operated by the Department of Energy, Office of Basic Energy Sciences. The SSRL Biotechnology Program is supported by the National Institutes of Health, National Center for Research Resources, Biomedical Technology Program, and by the Department of Energy, Office of Biological and Environmental Research. Its contents are solely the responsibility of the authors and do not necessarily reflect the opinions of the NIEHS, NIH, EPA, NSF or the DOE.

Thanks is also given to Porex Technology for the donation of the porous UHMW polypropylene sheet that was used to make the bed supports for the flow cells.

## REFERENCES

Brown, G.E. Jr., Calas, G., Waychunas, G.A., and Petiau, J. 1988, X-ray absorption spectroscopy and its applications in mineralogy and geochemistry, *in* Hawthorne, F.C., ed., Spectroscopic Methods in Mineralogy and Geology, Reviews in Mineralogy, v.18, p. 431-512.

Covington, A.K., Cressey, T., Lever, B.G., and Thirsk, H.R., 1962, Standard potential of the  $\beta$ -manganese dioxide electrode, Transactions of the Faraday Society, v. 50, p. 1975-1988.

Crowther, D.L., Dillard, J.G., and Murray, J.W., 1983, The mechanism of Co(II) oxidation on synthetic birnessite, *Geochimica et Cosmochimica Acta*, v. 47, p. 1399-1403.

Eychaner, J.H. and Stollenwerk, K.G., 1985, Neutralization of acidic ground water near Globe, Arizona, *in* Schmidt, K.D., ed., Groundwater Contamination and Reclamation, Proceedings of a symposium, Tucson, Arizona, 1985: Bethesda, MD, American Water Resources Association, p. 141-148.

Eychaner, J.H. 1991, The Globe, Arizona, research site -- Contaminants related to copper mining in a hydrologically integrated environment, *in* Mallard, G.E. and Aronson, D.A., eds., U.S. Geological Survey Toxic Substances Hydrology Program-- Proceedings of the technical meeting, Monterey, California, 1991, Water-Resources Investigations Report 91-4034, U.S. Geological Survey, Reston, VI, p. 439-447.

George, G., 1995, EXAFSPAK: A suite of computer programs for analysis of X-ray absorption spectra, Stanford Synchrotron Radiation Laboratory, Stanford, CA, p. 63.

Giovanoli, R., Feitknecht, W. and Fischer, F., 1971, Reduktion von mangan(III)-manganat(IV) mit zimtalkohol, *Helvetica Chimica Acta*, v. 54, p. 1112-1124.

Hem, J., 1980, Redox coprecipitation mechanisms of manganese oxides, *in* Kavanaugh, M.C., and Leckie, J.O., Particulates in Water, Advances in Chemistry Series, American Chemical Society, Washington, D.C., v. 189, p. 45-72.

Jardine, P.M. and Taylor, D.L., 1995, Kinetics and mechanisms of Co-EDTA oxidation by pyrolusite, *Geochimica et Cosmochimica Acta*, v. 59, no. 20, p. 4193-4203.

Kozawa, A. and Yeager, J.F., 1965, The cathodic reduction mechanism of electrolytic manganese dioxide in alkaline electrolyte, *Journal of the Electrochemical society*, v. 112, no. 10, p.959-963.

Lind, C.J., and Stollenwerk, K.G., 1995, Alteration of alluvium of Pinal Creek, Arizona, by acidic ground water resulting from copper mining, *in* Morganwalp, D.W. and Aronson, D.A., eds., U.S. Geological Survey Toxic Substances Hydrology Program – Proceedings of the Technical Meeting, Colorado Springs, Colorado, September 20-24, 1993. U.S. Geological Survey Water-Resources Investigations Report, 94-4015.

Lytle, F.W., Sandstrom, D.R., Marques, E.C., Wong, J., Spiro, C.L., Huffman, G.P., and

- Huggins, F.E., 1984, Measurement of soft x-ray absorption spectra with a fluorescent ion chamber detector, *Nuclear Instruments and Methods in Physics Research*, v. 226, p. 542-548.
- Nesbitt, H.W., Canning, G.W., and Bancroft, G.M., 1998, XPS study of reductive dissolution of 7 A-birnessite by  $\text{H}_3\text{AsO}_3$ , with constraints on reaction mechanism, *Geochimica et Cosmochimica Acta*, v. 62, no. 12, p. 2097-2110.
- Perez-Benito, J.F., Arias, C. and Amat, E., 1996, A kinetic study of the reduction of colloidal manganese dioxide by oxalic acid, *Journal of Colloid and Interface Science*, v. 177, p. 288-297.
- Qi-wu, W., and Wong, J., 1984, Mn valence and Mn-O bond length in  $\text{La}_{0.7}\text{A}_{0.3}\text{MnO}_3$  perovskite catalysts (A = Ca, Sr, Ba, and Pb), *in* Hodgson, K.O., Hedman, B. and Penner-Hahn, J.E., eds., *EXAFS and Near Edge Structure III: Proceedings of an international Conference*, Stanford, CA, July 16-20, 1984, Springer Verlag, New York, p. 202-205.
- Stahl, R.S., and James, B.R., 1991, Zinc sorption by manganese-oxide-coated sand as a function of pH, *Soil Science Society of America Journal*, v. 55, p. 1291-1294.
- Stollenwerk, K.G., 1994, Geochemical interactions between constituents in acidic groundwater and alluvium in an aquifer near Globe, Arizona, *Applied Geochemistry*, v. 9, p. 353-359.
- Todd, K.T., 1980, *Groundwater Hydrology*, second edition, John Wiley and Sons, New York, p. 28.
- Van Genuchten, M.Th. and Wierenga, P. J., 1976, Mass transfer studies in sorbing porous media, I, Analytical solutions, *Journal of the Soil Science Society of America*, v. 40, p. 473-480.
- Villinski, J.E., O'Day, P.A. and Conklin, M.H., 2000, Evidence for step-wise reduction of  $\text{MnO}_2$  by Fe(II): Results from an *in situ* real-time X-ray absorption spectroscopy experiment, in preparation.
- Wong, J., Koch, E.F., Henja, C.I., and Garbaskas, M.F., 1985, Atomic and microstructural characterizations metal impurities in synthetic diamonds, *Journal of Applied Physics*, v. 58, p. 3388-3393.

## AUTHOR INFORMATION

John E. Villinski (john@hwr.arizona.edu), Timothy L. Corely and Martha H. Conklin, The Department of Hydrology and Water Resources, The University of Arizona, Tucson, AZ, USA, 85721-0011.

Peggy A. O'Day, Geology Department, Arizona State University, Tempe, AZ, USA 85287-1404.